

Article

PacBio Sequencing Reveals Identical Organelle Genomes between American Cranberry (*Vaccinium macrocarpon* Ait.) and a Wild Relative

Luis Diaz-Garcia ^{1,2,*}, Lorraine Rodriguez-Bonilla ¹, Jessica Rohde ¹, Tyler Smith ³ 
and Juan Zalapa ^{1,4,*}

¹ Department of Horticulture, University of Wisconsin, Madison, WI 53705, USA; rodriguezbon@wisc.edu (L.R.-B.); jrohde4@wisc.edu (J.R.)

² Instituto Nacional de Investigaciones Forestales, Agrícolas y Pecuarias, Pabellon de Arteaga, Aguascalientes 20676, Mexico

³ Agriculture and Agri-Food Canada, Ottawa, ON K1A 0C6, Canada; tyler.smith3@canada.ca

⁴ USDA-ARS, Vegetable Crops Research Unit, University of Wisconsin, Madison, WI 53705, USA

* Correspondence: diaz.antonio@inifap.gob.mx (L.D.-G.); jezalapa@wisc.edu (J.Z.)

Received: 12 March 2019; Accepted: 3 April 2019; Published: 10 April 2019



Abstract: Breeding efforts in the American cranberry (*Vaccinium macrocarpon* Ait.), a North American perennial fruit crop of great importance, have been hampered by the limited genetic and phenotypic variability observed among cultivars and experimental materials. Most of the cultivars commercially used by cranberry growers today were derived from a few wild accessions bred in the 1950s. In different crops, wild germplasm has been used as an important genetic resource to incorporate novel traits and increase the phenotypic diversity of breeding materials. *Vaccinium microcarpum* (Turcz. ex Rupr.) Schmalh. and *V. oxycoccos* L., two closely related species, may be cross-compatible with the American cranberry, and could be useful to improve fruit quality such as phytochemical content. Furthermore, given their northern distribution, they could also help develop cold hardy cultivars. Although these species have previously been analyzed in diversity studies, genomic characterization and comparative studies are still lacking. In this study, we sequenced and assembled the organelle genomes of the cultivated American cranberry and its wild relative, *V. microcarpum*. PacBio sequencing technology allowed us to assemble both mitochondrial and plastid genomes at very high coverage and in a single circular scaffold. A comparative analysis revealed that the mitochondrial genome sequences were identical between both species and that the plastids presented only two synonymous single nucleotide polymorphisms (SNPs). Moreover, the Illumina resequencing of additional accessions of *V. microcarpum* and *V. oxycoccos* revealed high genetic variation in both species. Based on these results, we provided a hypothesis involving the extension and dynamics of the last glaciation period in North America, and how this could have shaped the distribution and dispersal of *V. microcarpum*. Finally, we provided important data regarding the polyploid origin of *V. oxycoccos*.

Keywords: American cranberry; domestication; organelle genomes; *Vaccinium*

1. Introduction

Worldwide, the majority of food crops derive from a few wild plant species. In the United States (USA), farmers grow a great variety of plants such as cereals, sugar crops, vegetables, and fruits (FAO, 2010). However, few crop species are native to North America, and even fewer can still be found in their wild forms and habitats. Wild germplasm, especially from crop wild relatives, is of tremendous

importance for breeding and agricultural production since it represents a pool of useful characteristics such as tolerance to biotic and abiotic stress, resistance genes, and traits influencing yield [1–4].

Vaccinium macrocarpon Ait. (American cranberry) is endemic to North America, and one of the few fruit crops that can still be found in the wild. The niche of this species is similar to its wild relative *Vaccinium oxycoccos* L. (small cranberry) [5–7]. However, *V. oxycoccos* is restricted to peatlands, where it grows embedded in moss lawns (usually sphagnum). *Vaccinium macrocarpon* grows in a wider variety of wetlands, including peatlands, swamps, and wet shores, and it will grow in mineral soils as well as moss lawns. *Vaccinium oxycoccos* produces over-wintering berries that, although smaller than the cultivated cranberry, share a similar flavor and possess a superior antioxidant content [8,9]. The high phytochemical content of the wild relative species and the relatively low genetic diversity in cultivated cranberry make the wild species extremely useful for breeding purposes [10,11]. In addition to its unique antioxidant profile, its northern and circumboreal distribution [12,13] make the small cranberry an interesting source of traits such as cold hardiness [14,15].

While the American cranberry is a diploid species, the small cranberry *V. oxycoccos* can be found as diploid, tetraploid, and, rarely, hexaploid forms. Although the most recent Flora of North America treatment [6] treats all three cytotypes as a single variable species (i.e., *V. oxycoccos*), morphological, molecular, phenological, and ecological data support the recognition of the diploid form as a distinct species: *Vaccinium microcarpum* (Turcz. ex Rupr.) Schmalh. [11,16,17]. According with [18], *V. macrocarpon* is considered the ancestral form, from which *V. microcarpum* was derived. According to this theory, the tetraploid *V. oxycoccos* formed following secondary contact of the diploid species through a combination of polyploidy and hybridization. He noted that this could have followed two paths: allopolyploid hybridization between *V. macrocarpon* and *V. microcarpum*, or the hybridization of autotetraploid plants derived from each diploid species. Regardless of the exact mechanism, he considered the morphology of *V. oxycoccos*, which is in some ways intermediate between the two diploids, strong evidence supporting hybrid ancestry. This hypothesis is supported by allozyme data [19], which shows that *V. oxycoccos* possesses alleles from both of the diploid species. However, the same data revealed no fixed heterozygous loci, which is consistent with tetrasomic inheritance as expected in autotetraploids [19,20]. Our own amplified fragment length polymorphism (AFLP) data [11] also reveal the presence of alleles from both diploids in *V. oxycoccos*, although simulation analysis suggests that it has diverged from the diploids since its formation. During the last decade, several studies regarding cranberry genetics and genomics have been published. In 2013, the first simple sequence repeat (SSR)-based genetic map was published, in which several quantitative trait loci (QTL) for yield-related traits and important phytochemicals were reported [21]. Subsequently, high-density genetic maps as well as more multi-trait QTL studies became available [22–27]. In addition, nuclear [28], plastid [29], and mitochondrial [30] genomes have been published recently. Regarding diversity between *V. macrocarpon* and wild relatives such as *V. microcarpum* and *V. oxycoccos*, most of the studies have been based on simple sequence repeat (SSR) markers generated from both nuclear and organelle genomes [31–35].

Given the recent advances on next-generation sequencing technologies, we generated PacBio complete plastid and mitochondrial genomes of an Alaskan accession of *V. microcarpum* as well as updated the American cranberry organelle genomes. A comprehensive comparison between the organelles of these two species revealed near identical sequences, which indicates common ancestry with implications about the origin of cultivated *V. macrocarpon* in North America. Moreover, Illumina resequencing in *V. microcarpum* samples collected in eastern Canada suggested a process of genetic diversification. Finally, we provided more evidence regarding the polyploid origin of *V. oxycoccos*.

2. Materials and Methods

2.1. Plant Material

For *V. macrocarpon*, we used the commercial cultivar “Stevens”, which was derived from a cross between two wild selections, “McFarlin” (from MA, USA) and “Potter’s Favorite” (from WI, USA).

For *V. microcarpum*, we used an accession collected by N. Vorsa (Rutgers University, New Brunswick, Newark and Camden, NJ, USA) in southern Alaska and described in Mahy et al. (2000). Both plants were maintained clonally under greenhouse conditions at the University of Wisconsin-Madison (Madison, WI, USA). These accessions have been extensively used in different marker studies, providing a unique genetic fingerprint based on nuclear and organellar information as well as known genetic relationships based on relatively diverse samples of *V. macrocarpon*, *V. microcarpum*, and *V. oxycoccus* [19,31–33]. In Figure 1, we show the distinctive plant characteristics and attributes of each of our *V. microcarpum* and *V. macrocarpon* accessions.



Figure 1. Distinctive characteristics of plant architecture and fruit of *V. microcarpum* and *V. macrocarpon* “Stevens” plants.

2.2. PacBio Sequencing, Genome Assembly, and Annotation

Young leaves of *V. macrocarpon* and *V. microcarpum* were processed at Amplicon Express (Pullman, WA, USA) to obtain high molecular weight DNA. Two single-molecule real-time (SMRT) cells of PacBio Sequel (Pacific Biosciences of California, Inc., CA, USA) were sequenced for each species at The DNA Technologies and Expression Analysis Cores of the University of California-Davis (Davis, CA, USA). For each species, a complete de novo assembly (including all the raw reads) was performed on Canu v1.7 [36] using the automatic pipeline (that includes read correction, trimming, and assembly) with default parameters. From these assemblies, mapping (using BLASTn) the plastid assembly published by Fajardo et al. (2013) allowed us to extract contigs of lengths 209,726 bp (for *V. macrocarpon*) and 223,859 bp (for *V. microcarpum*), which we believed contain the complete plastid genomes. On the other hand, mapping the reference mitochondrial genome published by Fajardo et al. (2014) yielded contigs with lengths smaller than the expected genome size (459,678 bp); therefore, an alternative strategy was carried out as follows. Raw PacBio reads were mapped with BlastR (with minMatch = 15, and fastSDP and advanceHalf activated) using as reference the mitochondrial genome published by Fajardo et al. (2014); then, filtered reads were de novo assembled using the automatic pipeline of Canu as in the assembling process used for the plastid. For *V. macrocarpon* and *V. microcarpum*, the largest contig on each assembly was 468,773 bp and 468,164 bp, respectively. Since Canu was ran using the default

parameters, all of the assemblies were resolved at $\sim 40\times$ coverage. As described in the user's manual, Canu processes the longer reads up to get $40\times$, which are further corrected using the remaining shorter reads. Thus, a conventional estimation of coverage (which is computed using all the reads) would be considerably larger than this. A round of polishing was performed in the plastid and mitochondrial assemblies of both species using Arrow (with default parameters). Subsequently, the circularity of each assembly was checked with the tool Circlator v1.5.5 [37] using `b2r_length_cutoff = 100,000` and `merge_reassemble_end = 9000`. Following the recommendations of Circlator's authors, a final round of polishing with Arrow was performed in all four assemblies, (i.e., two organelles each for *V. macrocarpon* and *V. microcarpum*).

Gene annotation was performed with GeSeq [38] using all the *Ericales* and *Asterids* as reference; the percentage of identity for the BLAT protein search, and for the BLAT rRNA, tRNA, and DNA search, were set to 70 and 80, respectively. All the annotations were manually reviewed and corrected, if necessary, in Geneious R11 [39]. GC content was analyzed in R [40] using the package Biostrings. SSR search was performed with Phobos version 3.3.12 [41].

2.3. Illumina Sequencing and Mapping

We extended our study by sequencing additional accessions of *V. macrocarpon* and *V. microcarpum*, as well the tetraploid species *V. oxycoccus*. For *V. macrocarpon*, we included samples WABL11, WC16-13 and WC16-16. For *V. microcarpum*, we include samples QCCW5, QCJB20, and QCWA9 (previously described in Smith et al., 2015). For *V. oxycoccus*, we include three wild samples: MWB3, PMS5 and PB17. Additionally, the *V. macrocarpon* and *V. microcarpum* samples used for PacBio sequencing were also sequenced with Illumina (San Diego, CA, USA). In Table 1, a summary of the samples used for both PacBio and Illumina sequencing as well as important information regarding their collection sites is provided.

Table 1. *Vaccinium* samples sequenced and assembled in this study.

Sample ID	Species	Collected from	Sequencing Technology
	<i>V. macrocarpon</i> (cultivar Stevens)	Madison, WI, USA	PacBio Sequel and Illumina
	<i>V. microcarpum</i>	Alaska, USA	
WABL11		Vilas County, WI, USA	
WC16-13	<i>V. macrocarpon</i>	North-Central WI, USA	Illumina
WC16-16		NJ, USA	
QCCW5	<i>V. microcarpum</i>	Quebec, ON, Canada	
QCJB20			
QCWA9			
MWB3	<i>V. oxycoccus</i>	Manitowish Waters, WI, USA	
PMS5			
PB17		Pennington, MN, USA	

Genomic DNA was extracted using NucleoSpin[®] Plant II (Macherey-Nagel, Bethlehem, PA, USA), and submitted to The Biotech Center at the University of Wisconsin-Madison (Madison, WI, USA) for sequencing. Indexed samples were evenly loaded into three HiSeq 2500 Illumina (San Diego, CA, USA) lanes, 1×100 bp. Illumina reads were cleaned using Trimmomatic [42] (minimum length 85 bp and minimum quality 28), and then mapped against our PacBio organelle genomes with bwa. Later, filtered reads were de novo assembled using Abyss with the parameter `k = 64`, and the contigs were ordered based on the organelle reference genomes in Geneious R11 (Newark, NJ, USA). Variants were searched first, by aligning all nine samples (global SNP across all nine species), and then by aligning the samples of the same species (specific alignments, three sequences per species). Alignments were performed using the progressive method implemented in Mauve [43]; SNP were called after masking gaps in the alignment.

2.4. Phylogenetic Analysis

Due to the recent increase in the availability of plastid genomes, especially from the *Ericales*, we carried out a phylogenetic analysis using 68 genes (five *atp* genes, *ccsa*, *cema*, *matk*, 11 *ndh*, six *pet*, five *psa*, 14 *psb*, *rbcl*, seven *rpl*, three *rpo*, 11 *rps*, and two *ycf*), which were consistently present in 69 plastid genomes. In this analysis, 36 genomes corresponded to the *Ericales*. All the genome sequences were downloaded from NCBI. Coding sequences were extracted in Geneious R11, and imported in R using the package Biostrings for filtering the genes present in the majority of the species. Then, gene sequences were concatenated for each species, exported in fasta format, and imported back in Geneious R11 for sequence alignment and tree construction. Alignments were performed using the progressive method implemented in MAFFT v7 [44] with the default parameters. Optimal trees were inferred using Maximum Likelihood as implemented in FastTree [45]. Since mitochondrial genomes of *Ericales* are still scarce, we did not perform any phylogenetic analysis based on mitochondrial sequences.

3. Results and Discussion

3.1. Cultivated and Wild Cranberries Share Identical Organelle Genomes

The first mitochondrial and plastid genomes in *V. macrocarpon* were published in 2014 [30] and 2013 [29], respectively. While these assemblies were highly reliable, the advantages of today's single molecule real-time sequencing allowed us to improve the current assemblies and generate novel organelle genomes of *V. microcarpum*.

The complete mitochondrial genome of *V. macrocarpon* obtained here was 468,115 bp long, which is almost 10 kb larger than the original version [30], while the plastid was 176,093 bp long—just 48 bp longer [29]. Both assemblies were resolved in a single circular scaffold with a mean coverage (based on PacBio corrected reads only) of 39.8× for the mitochondria, and 38.9× for the chloroplast. For the mitochondria, the GC content was very similar with the previous version (45.3% versus 45.4%), whereas for the plastid, the GC content was identical for both versions (36.8%). Moreover, the GC content in both organelles fell within the expected range of the *Asterids* clade (based on the mitochondrial genomes for this group available in NCBI). To identify major structural changes between previous and current assemblies of *V. macrocarpon* organelles, we performed whole-genome alignments using MuMmer [46] (Figure 2). For the mitochondrial genome, 376 rearrangements were observed; from those, 50% corresponded to sequences smaller than 30 nucleotides, and 81% corresponded to sequences smaller than 100 nucleotides. Although MuMmer identified rearrangements involving large sequences, they (and most of the smaller ones) shared perfect synteny between previous and current genome assemblies. For the plastid genome, 161 rearrangements were observed, from which 17% involved sequences smaller than 30 nucleotides and 43% involved sequences smaller than 100 nucleotides. Similar to the mitochondrial genome, most of the rearrangements did not affect the overall synteny between both assemblies.

For *V. microcarpum*, the genomes were resolved in a single circular scaffold with a mean coverage of 37.1% and 39.5% for mitochondrial and plastid genomes, respectively. Remarkably, both the mitochondrial and plastid genomes of *V. microcarpum* were completely identical to the ones in *V. macrocarpon*, with an exception of two synonymous single nucleotide polymorphisms (SNPs) in the plastid, which are described below. Illumina resequencing of both *V. macrocarpon* and *V. microcarpum* confirmed our PacBio assemblies. Both organelle genome assemblies for *V. macrocarpon* and *V. microcarpum* were deposited in the GenBank (MK715444, MK715445, MK715446, and MK715447).

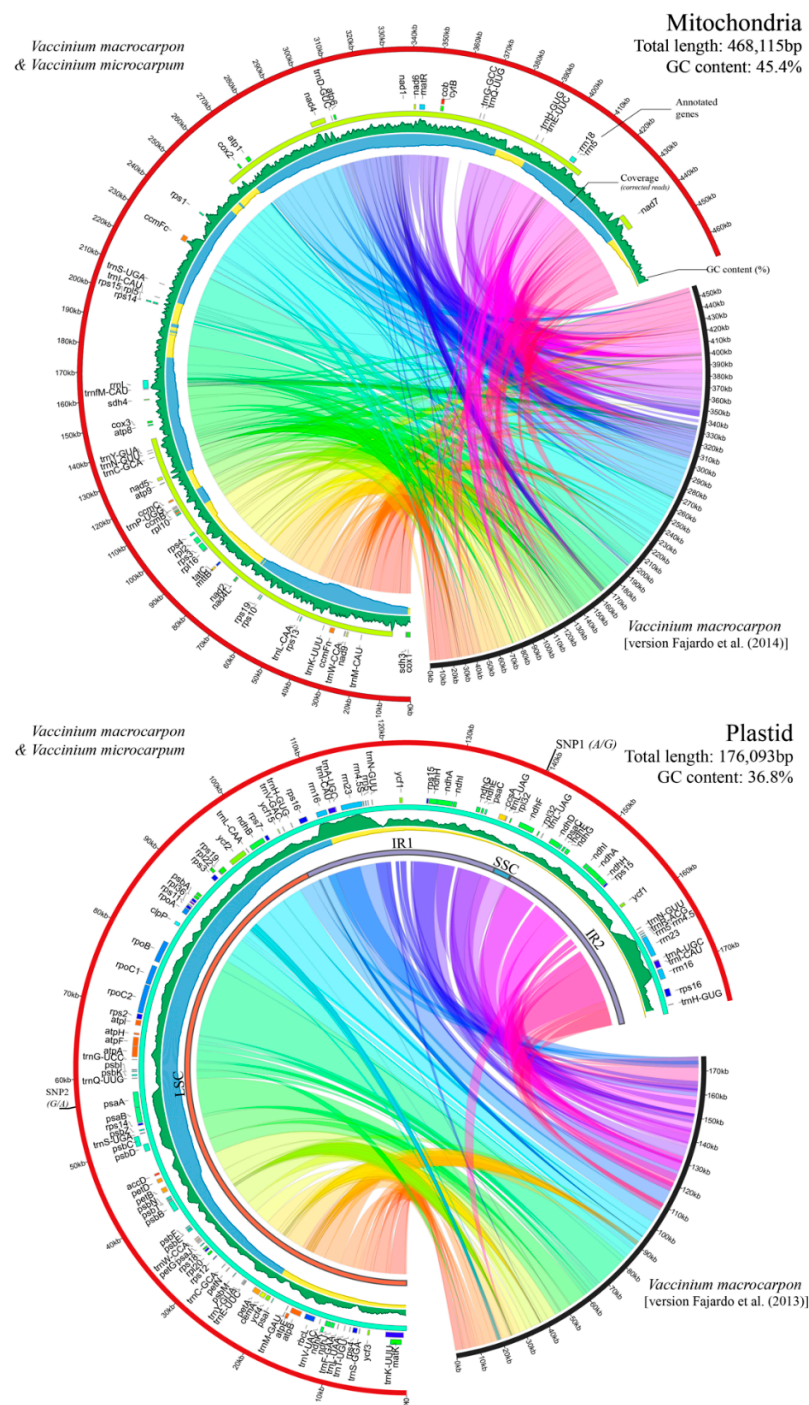


Figure 2. Organelle genomes of *V. macrocarpon* and *V. microcarpum*. A comparison between the PacBio assemblies presented in this study and previously published cranberry organelle versions [29,30] are shown; collinear regions were calculated using MuMmer with default parameters (see Materials and Methods). Since *V. macrocarpon* and *V. microcarpum* presented near-identical organelles, for the plastid genome, only single nucleotide polymorphism (SNP) positions are provided, and the mitochondria shown are identical. Gene annotations are shown as tiles in internal tracks; colors were randomly assigned to highlight different categories of protein-coding genes, ribosomal RNA and tRNA. Sequencing coverage is provided in area plots oriented inwards, where blue, yellow, and red represent genome areas with $>30\times$, $>10\times$, and $\leq 10\times$ coverage, respectively (based on PacBio corrected reads). GC content is also provided as a green-colored area plot. In the plastid, large single copy (LSC), small single copy (SSC), and inverted repeats (IR1 and IR2) are highlighted with red, blue, and purple concentric bars.

Although uncommon, several studies in other plant species have reported the similarity of organelle genomes among cultivated and wild species. For example, the mitochondrial genomes of wild (*Hordeum vulgare* ssp. *spontaneum*) and cultivated (*H. vulgare* ssp. *vulgare*) barley, which has a history of 10,000 years since its domestication from the wild progenitor, are identical with the exception of three SNPs [47]. Similarly, a study regarding plastid inheritance in *Nicotiana tabacum* found very few SNPs when comparing the latter with *N. sylvestris*, its maternal wild progenitor [48].

3.2. Genome Architecture and Gene Content

Since *V. macrocarpon* and *V. microcarpum* contained near-identical organelle genomes, the following results regarding gene content, repeated sequences, and other statistics apply for both species.

For the mitochondria, gene content was similar to the previous genome version [30]. We found nine genes of the respiratory chain complex I (nad-NADH dehydrogenase), two of the complex II (sdh-succinate oxido-reductase, one more than in Fajardo et al. (2014)), one of the complex III (apocytochrome b), three of the complex IV (cox-cytochrome oxidase), and five of the complex V (atp-ATP synthase, one more than in [30]). In addition, we found four genes of the cytochrome c biogenesis (ccm), two for the cytochrome b (cytB and petL), one transcription gene (mat-maturase), one transporter protein (mtt-B), three ribosomal RNA (rrm), 13 ribosomal proteins (rpl and rps genes), and a malonate uptake protein (tatC). In total, we found 17 tRNA, from which three were duplicated (trnL, trnM, and trnS). In Fajardo et al. (2014), the authors reported the presence of two copies of tRNA-Sec, which is an unusual transfer RNA in land plants; here, we confirm its presence, but in a single copy (exon 1 of copy 1 (located at ~45 kb) has a single different nucleotide). Out of the 42 protein-coding genes found in the mitochondrial genome, three contained non-ATG start codons, and eight had undetermined stop codons (different than TAA, TGA, or TAG). Among these, the gene petL had both start and stop codons undetermined; it was also 73 nucleotides long. Similarly, gene mttB was expected to have a non-ATG start codon based on previous studies [49–52]. Protein-coding genes varied largely in size and intervals, ranging from a few hundred nucleotides and a single interval (one exon), to thousands of nucleotides and up to five intervals (i.e. *nad7* and *nad2*). Regarding SSR, we observed 1449 motifs with total lengths ranging from six to 26 nucleotides. As expected, dinucleotides and trinucleotides were the most abundant (80.0% and 15.6%, respectively); tetra, penta, and hexanucleotides account for less than 5%. The repeat AG was the most abundant motif among the dinucleotides. A complete list of repeated sequences in the mitochondria is provided in Supplementary File 1.

Most of the genes found in the plastid were also consistent with the previous version published by Fajardo et al. (2013). The annotated sequences were classified as follows: out of the 68 unique protein-coding genes, six corresponded to ATP synthase subunits (atp genes), 11 corresponded to NADH-dehydrogenase subunits (ndh genes), six corresponded to cytochrome b/f complex subunits (pet genes), five corresponded to photosystem I subunits (psa genes), 16 corresponded to photosystem II subunits (psb genes), eight corresponded to large ribosomal protein units (rpl genes), 12 corresponded to small ribosomal protein units (rps genes), and four corresponded to RNA polymerase subunits (rpo genes). Other important genes such *accD*, *ccsA*, *infA*, *matK*, and *rbcL* were also found. More than 95% of these genes showed regular start and stop codons. Five hypothetical genes (*ycf*) were found, although only one showed standard start and stop codons. In addition, four ribosomal RNA and 26 unique transfer RNA were found. The length of the large single copy (LSC), small single copy (SSC), and inverted repeats (IR) fragments were 104,592 bp, 3025 bp, and 34,238 bp, respectively. All the ribosomal RNA were located in the IR; therefore, two copies of each gene were found. On the other hand, *ndhF* was the only gene in the SSC. Only 492 SSRs were found in the plastid genome with the following proportions: dinucleotide 77.2%, trinucleotide 13.4%, tetranucleotide 5.9%, and both penta and hexanucleotide with less than 2.0% each. The dinucleotide motif AT was the most abundant (Supplementary File 1). SSR frequency and the distribution of SSR motif type were different compared with previous studies in cranberry [33]. In the previous study, the mitochondria had fewer

SSR (one every 3.8 kb) than the plastid (one every 2.0 kb) genome (in average), and the tetranucleotide motifs were the predominant for both organelle genomes.

As mentioned before, both mitochondrial and plastid genomes were virtually identical between *V. macrocarpon* and *V. microcarpum*. Only two SNPs were found in the plastid; the first one (G in *V. microcarpum*, A in *V. macrocarpon*, at position 139,582 bp) was located in the *ndhF* (at the SSC fragment), and was a non-synonymous mutation producing isoleucine in *V. macrocarpon* and valine in *V. microcarpum*, which were two similar non-polar aminoacids. The second SNP (A in *V. microcarpum*, G in *V. macrocarpon*, at position 57,591 bp) was located in the *psaA* gene, and it resulted in a synonymous change (which was translated to the amino acid glycine in both cases).

3.3. Phylogenetic Analysis of *V. macrocarpon* and Related Species

To study the phylogenetic position of *V. macrocarpon* within the Ericales, we performed an analysis based on 68 genes consistently present among 36 Ericales genomes, and 39 from other families (Figure 3). As expected, the Ericales formed a monophyletic group. The topology of our tree mirrors relationships recovered from a more comprehensive analysis of a supermatrix that includes nearly 5000 species and 25 loci [53]. In both analyses, the balsaminoids (represented by *Impatiens piufanensis* and *Hydrocera triflora* in our data) are placed sister to the rest of the Ericales; the Ericaceae are sister to the sarracenioids (represented by *Actinidia* in our data) in a strongly supported clade. Our data included two additional Ericaceae: *Arbutus unedo* and *Chamaedaphne calyculata*. Of these, *V. macrocarpon* was most closely related to *C. calyculata*. *Chamaedaphne calyculata*, which is a circumboreal species with a recently published plastid genome [54], shares almost an identical genome architecture with *V. macrocarpon*, with the most profound changes in the inverted repeat regions. Moreover, *C. calyculata* shares many phenotypic traits with wild *V. macrocarpon* plants [55].

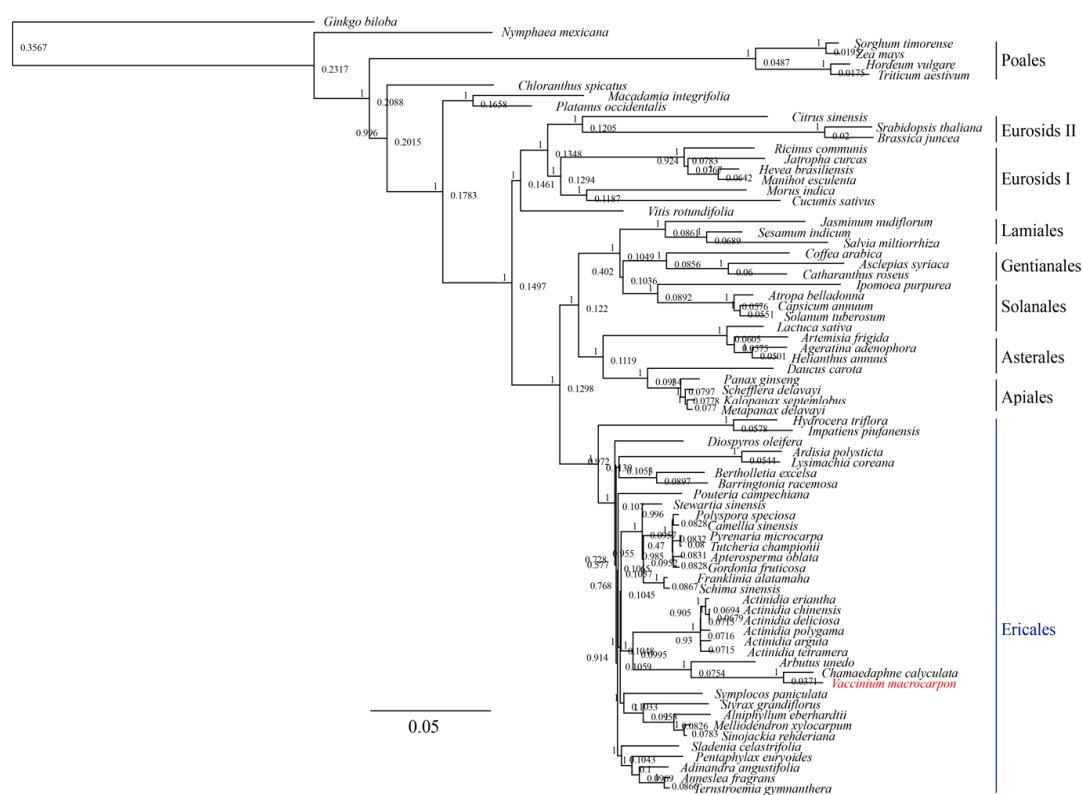


Figure 3. Phylogenetic relationship of *V. macrocarpon* (and Alaskan *V. microcarpum*) with related species based on 68 protein-coding genes shared by all the plastid genomes. Tree constructed in FastTree using the generalized time-reversible (GTR) model. Branch labels correspond to the FastTree support values, whereas node labels show node heights. *Ginkgo biloba* was used as the outgroup.

3.4. Divergent *V. microcarpum* Can Be Found in Eastern Canada

Due to the remarkable similarity found between *V. macrocarpon* and *V. microcarpum* organelle genomes, we expanded our study by resequencing additional accessions from a broader geographic area. In particular, we included samples of *V. microcarpum* collected in Quebec, Canada, *V. oxycoccus* (4×) collected in Wisconsin and Minnesota, USA, as well as *V. macrocarpon* from Wisconsin and the east coast of the USA (Table 1). For these samples, Illumina resequencing allowed us to partially assemble both mitochondrial and plastid genomes at a very high coverage (>1000×). After removing contigs smaller than 5 kb, mitochondrial genome assemblies for all nine samples had a length between 394–428 kb distributed among 27–30 scaffolds (additional statistics regarding assemblies are provided in Supplementary File 1). For the plastid, assembly lengths (taking in account only one of the inverted repeats) ranged from 76–95 kb among 7–10 contigs. The incompleteness of these de novo assemblies could have been produced by two main causes. First, the use of very short reads (1 × 100 bp) could have hampered the assembly process. Second, since these de novo assemblies were conducted using a subset of raw reads that mapped to our *V. macrocarpon* PacBio assembly, potential novel sequences absent in either the reference or the additional accession could have been missed. After orienting and ordering the plastid and mitochondrial contigs for all nine samples (based on *V. macrocarpon*), we aligned them and identified SNP variants. By considering aligned and ungapped regions involving all nine samples (using our *V. macrocarpon* PacBio assemblies as reference), we discovered 831 SNPs in the mitochondria (Figure 4A and Table 2) and 121 in the plastid (Figure 4B and Table 2). Of the SNPs found in the mitochondrial genome, four were located in the *nad1* gene, 15 were located in the *nad2* gene, and one was located in the *rps14* gene. In the plastid, 39 SNPs were found in 13 different genes, in which *ycf2* had the most (11). A large portion of SNPs was found in the regions delimiting the inverted repeat regions, which was expected given their volatility [56]. When aligning only the wild *V. macrocarpon* samples, 10 SNPs were found in the mitochondria and 11 were found in the plastid (Figure 4C, top panel). Similarly, alignments of only the tetraploid *V. oxycoccus* resulted in 11 SNPs each for both mitochondria and plastid (Figure 4C, bottom panel). In contrast, the alignment of the Canadian *V. microcarpum* samples resulted in 232 SNPs in the mitochondria and 332 SNPs in the plastid; from these, more than 95% of the SNPs were called, because sample QCWA9 showed alternative alleles (Figure 4C, middle panel; for space reasons, only the first alignment position is shown).

Table 2. Proportion of *V. oxycoccus* SNPs found in either *V. macrocarpon*, *V. microcarpum*, or that represent novel alleles.

Origin of the SNP	Mitochondria		Plastid	
	Counts	Percentage	Counts	Percentage
<i>V. macrocarpon</i>	827	99.3%	33	26.4%
Private <i>V. oxycoccus</i> Alleles	5	0.4%	22	17.4%
<i>V. microcarpum</i>	1	0.1%	67	55.4%
Total	833	100%	122	100%

Additionally, we carried out an alternative approach in which, instead of comparing the *de novo* assemblies, the Illumina raw reads (previously trimmed and cleaned) were directly mapped using our *V. macrocarpon* as reference, and low coverage regions were recorded. This strategy revealed that the mitochondrial genomes of the wild *V. macrocarpon* samples WC16-13 and WC16-16 were very similar to our reference; however, we could not find Illumina reads of WABL11 to map a ~1 kb region at position ~198 kb of our *V. macrocarpon* assembly. Also, when mapping mitochondrial raw reads of our Canadian *V. microcarpum* samples, we observed a region of ~8 kb at position ~55 kb, and a two-interval region of ~7 kb at position ~384 kb in which we could not find Illumina reads to map. Interestingly, all the *V. oxycoccus* (4×) samples showed a continuous and ungapped coverage along both plastid and mitochondrial genomes. Figure 4D shows the unique coverage plots observed across all nine samples

in the mitochondria; in Figures S1 and S2, all the coverage maps for both mitochondria and plastid genomes are provided.

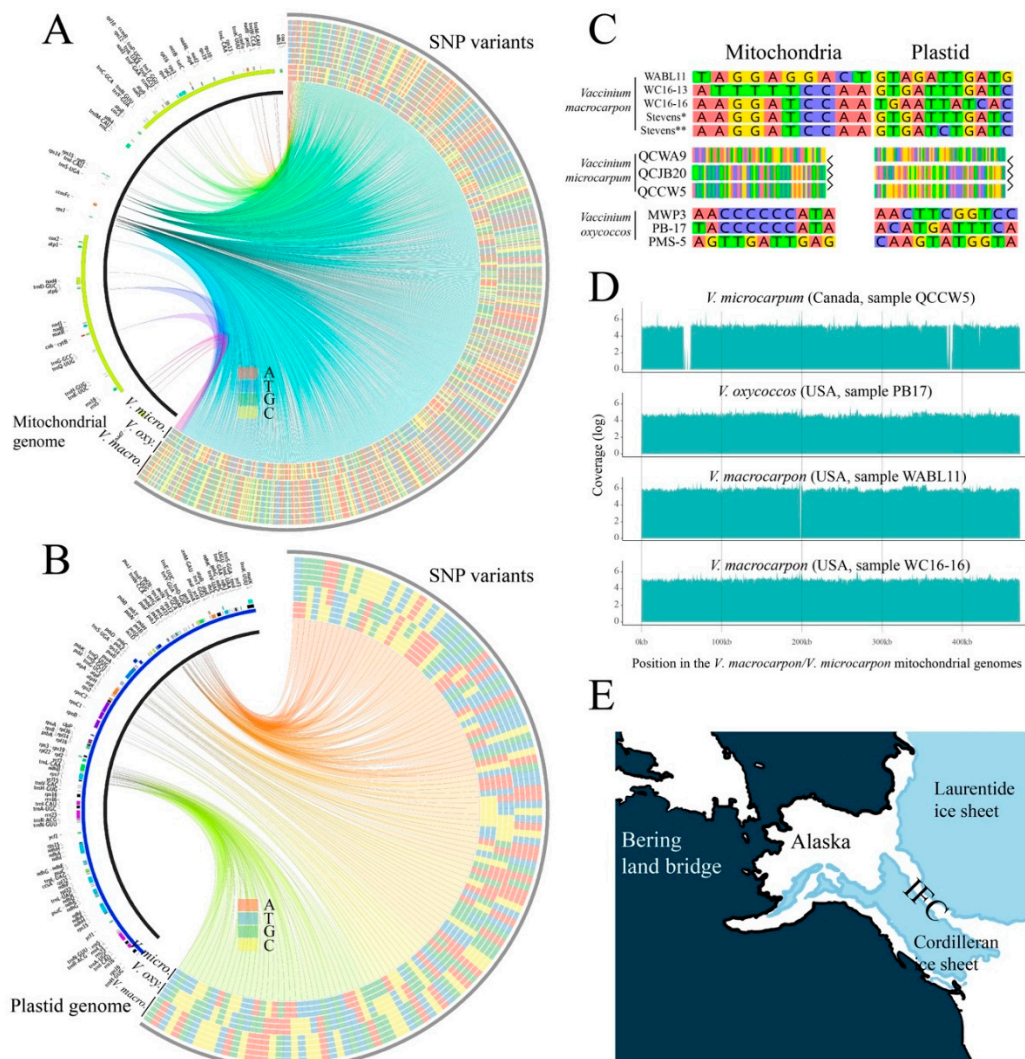


Figure 4. SNP variants among *V. macrocarpon*, *V. microcarpum*, and *V. oxycoccus*. SNP (single nucleotide polymorphism) variants detected in mitochondria (A) and plastid (B) genomes among all 11 samples sequenced with both Illumina and PacBio. On the heatmaps (right arcs), the inner three rings correspond to the *V. microcarpum* samples QCCW5, QCJB20, and QCWA9; the next three rings (4–6) correspond to the *V. oxycoccus* samples MWPB3, PB17, and PMS5; rings 7–9 correspond to the wild *V. macrocarpon* samples WABL11, WC16-13, and WC16-16; and rings 10–11 correspond to cultivated *V. macrocarpon* sequenced with Illumina and PacBio, respectively (note these last two sequences were identical to the Alaskan *V. microcarpum* sequences). Each SNP is connected by a colored link to its physical position within either the mitochondria or plastid genome (left to right arcs); link colors are meaningless. For reference purposes, gene locations were added on the left arcs and colored by category. (C) SNP variants were called when aligning sequences by species; for the *V. macrocarpon* alignment, Stevens* correspond to the assembly carried out with Illumina data (used to validate the PacBio assembly), whereas Stevens** correspond to the one with PacBio; for *V. microcarpum*, only the first positions of the alignment are shown. (D) Coverage plots using Illumina filtered raw reads and *V. macrocarpon/V. microcarpum* mitochondrial genomes as reference (additional coverage plots are provided in Figures S1 and S2). (E) Ice extent between 9–10 k years ago showing the ice-free corridor (IFC).

3.5. Relationships among Diploids, and the Link between Alaskan *V. microcarpum* and *V. macrocarpon*

Vaccinium macrocarpon and *V. microcarpum* displayed dramatically different genetic diversity. Our samples of *V. macrocarpon* span 1700 km from Wisconsin to the east coast. Despite the geographic distance, four samples yielded only 21 intraspecific SNPs combined for the chloroplast and mitochondrial genomes. In contrast, we found 564 intraspecific SNPs in three *V. microcarpum* samples collected within 260 km along the James Bay Coast. This is a very modest representation of a species with a circumboreal distribution; more comprehensive sampling is likely to reveal further diversity.

The organelle genomes shared by the Alaskan *V. microcarpum* sample and all the *V. macrocarpon* samples was surprising. Given the unexpected diversity in our *V. microcarpum* plants, this could be explained by the persistence of multiple ancestral cytoplasmic lineages across the range of *V. microcarpum*, including the one now present in *V. macrocarpon*. In other words, the shared genomes are the consequence of incomplete lineage sorting among *V. macrocarpon* and *V. microcarpum*.

Alternatively, the shared genomes could be the result of past gene flow between the Alaskan *V. microcarpum* populations and *V. macrocarpon* in eastern North America. Our *V. macrocarpon* accession was collected in southern Alaska, in the region of the ice-free corridor (IFC) that connected eastern Alaska with the north-central region of the USA during the deglaciation period between 8000–11,000 years (Figure 4E) [57]. The IFC enabled the movement of humans and wildlife across the continent thousands of years before the Laurentide ice sheet retreated from eastern Canada, which could explain the closer genetic relationship between *V. macrocarpon* and the Alaskan *V. microcarpum* than that of the geographically closer populations in Quebec. Further sampling across the range of *V. microcarpum* is needed to clarify this situation.

3.6. The Origin of the Tetraploid *V. oxycoccus*

Different studies have discussed the tetraploid origin of *V. oxycoccus*, but no definitive answer has been provided. Two main theories have been proposed. The first one describes that *V. oxycoccus* arose as a hybrid of the two diploid taxa, *V. macrocarpon* and *V. microcarpum* [18], whereas the second suggests that *V. oxycoccus* is most likely the autopolyploid descendant of the diploid *V. microcarpum* [19]. Since *V. oxycoccus* was included in our resequencing analysis, the SNPs found across all three species may provide evidence regarding the origin of *V. oxycoccus*.

For 827 of the 831 mitochondrial SNPs (99.3%), *V. macrocarpon* and *V. oxycoccus* shared the same allele (Table 2). *Vaccinium oxycoccus* and *V. microcarpum* shared the same allele at a single mitochondrial SNP (<1%). This strong link to *V. macrocarpon* refutes the hypothesis that *V. oxycoccus* is an autopolyploid descendant of *V. microcarpum*. The simplest explanation is that *V. oxycoccus* is an allotetraploid, and that *V. macrocarpon* was the ancestral cytoplasmic donor.

However, the chloroplast data challenges this simple explanation, as the *V. oxycoccus* genome appears to contain a mixture alleles from both diploid species. *Vaccinium macrocarpon* and *V. microcarpum* are distinguished by 100 chloroplast SNPs. Of these, *V. oxycoccus* had the “*microcarpum*” allele for 67 SNPs, and the “*macrocarpon*” allele for 33 SNPs. We are not aware of any mechanism that would enable recombination between chloroplast genomes from diploid ancestors to yield a mixture of genomes in the derived polyploid. This may indicate that our sampling was not adequate to capture the full scope of variation in the chloroplast genomes among the three species. That is, the alleles that are unique to *V. macrocarpon* and *V. microcarpum* in our data may actually be present in both species. Alternatively, a third diploid species may have been involved in the formation of tetraploid *V. oxycoccus*.

The possible existence of undocumented genetic diversity is further supported by the contrasting results from the PacBio sequencing. These data show that the Alaskan *V. microcarpum* sample possesses mitochondrial and chloroplast genomes that are identical to *V. macrocarpon*, and markedly different from the genomes of conspecific samples from Quebec. This could be explained by the preservation of multiple ancestral organelle lineages in the circumboreal *V. microcarpum*, including the one present in the more geographically restricted *V. macrocarpon*.

Alternatively, it could be an indication of cryptic variation in the *V. oxycoccus/V. microcarpum* group. In this context, it has been recognized the existence of a western cranberry species (*Oxycoccus ovalifolius* (Michx.) Porsild) [58], however, later authors have subsumed it within *V. oxycoccus* (along with *V. microcarpum*, [5]). Moreover, genetic studies of *V. microcarpum* have been geographically limited: Mahy et al. (2000) included only Alaskan *V. microcarpum* samples, and Smith et al. (2015) was restricted to western Quebec. The results of the current study suggest that a broader assessment of genetic diversity in diploid cranberries across their northern range may reveal taxonomically and agronomically valuable variation.

3.7. Conclusions and Further Directions

Our study of the organelle genome architecture of *V. macrocarpon*, *V. microcarpum*, and *V. oxycoccus*, and their diversity across North America, revealed a remarkable similarity between the cytoplasm of Alaskan *V. microcarpum* and cultivated *V. macrocarpon*. Moreover, we showed that a highly differentiated *V. microcarpum* can be found in eastern Canada, and suggested that the spatial and temporal dynamics of the last glaciation period could have shaped the genetic diversity among cranberry species. Further studies should investigate the genomic rearrangements observed in Canada's *V. microcarpum* samples as well as elaborate a more extensive sampling and genomic profiling of germplasm across Alaska and the "ice-free corridor". In summary, this study provided important insights about the movement and genetic differentiation of cranberry and its wild relatives in North America, which is of vital importance for the inclusion of wild germplasm into cranberry breeding programs.

Supplementary Materials: The following are available online at <http://www.mdpi.com/2073-4425/10/4/291/s1>. Supplementary File 1: Additional datasets; Figure S1: Coverage maps for mitochondrial genomes; Figure S2: Coverage maps for chloroplast genomes.

Author Contributions: Conceptualization, L.D.-G. and J.Z.; Data curation, L.R.-B. and J.R.; Formal analysis L.D.-G., L.R.-B. and T.S.; Methodology, L.D.-G., L.R.-B., J.R. and J.Z.; Project administration, J.Z.; Resources, T.S. and J.Z.; Visualization, L.D.-G.; Writing—original draft, L.D.-G., L.R.-B., T.S. and J.Z.; Writing—review & editing, L.D.-G., L.R.-B., T.S. and J.Z.

Funding: This project was supported by USDA-ARS (project no. 5090-21220-004-00-D provided to JZ); WI-DATCP (SCBG Project #14-002); Ocean Spray Cranberries, Inc.; Wisconsin Cranberry Growers Association; Cranberry Institute. LDG was supported by the Consejo Nacional de Ciencia y Tecnología (Mexico) and the Gabelman-Seminis Graduate Fellowship. LRB was supported by the UW Madison SciMed GRS.

Acknowledgments: We are grateful to Drs. Mike Havey and Sean Schoville at UW-Madison for their helpful insight. Also, we want to thank the Wisconsin and Minnesota Department of Natural resources for the permits to collect in their lands as well as the US Forest Service. J.Z. would like to express his gratitude through Ps 136:1. The authors also thank the anonymous reviewers who helped enhance the quality of this paper.

Conflicts of Interest: The authors declare no conflict of interest.

References

1. Dempewolf, H.; Baute, G.; Anderson, J.; Kilian, B.; Smith, C.; Guarino, L. Past and Future Use of Wild Relatives in Crop Breeding. *Crop Sci.* **2017**, *57*, 1070–1082. [CrossRef]
2. Hajjar, R.; Hodgkin, T. The use of wild relatives in crop improvement: A survey of developments over the last 20 years. *Euphytica* **2007**, *156*, 1–13. [CrossRef]
3. Jarvis, A.; Lane, A.; Hijmans, R.J. The effect of climate change on crop wild relatives. *Agric. Ecosyst. Environ.* **2008**, *126*, 13–23. [CrossRef]
4. Maxted, N.; Kell, S.; Ford-Lloyd, B.; Dulloo, E.; Toledo, Á. Toward the Systematic Conservation of Global Crop Wild Relative Diversity. *Crop Sci.* **2012**, *52*, 774–785. [CrossRef]
5. Vander Kloet, S.P. The taxonomy of *Vaccinium* section *Oxycoccus*. *Rhodora* **1983**, *85*, 1–43.
6. Vander Kloet, S.P. *Vaccinium* Linnaeus. In *Flora N. Am. North Mexico, Vol. 8: Magnoliophyta: Paeoniaceae to Ericaceae*; Morin, N.R., Ed.; Oxford University Press: New York, NY, USA, 2009; pp. 515–530.
7. Vorsa, N.; Johnson-Cicalese, J. American cranberry. *Fruit Breed.* **2012**, *8*, 191–223.
8. Jacquemart, A.-L. *Vaccinium Oxycoccus* L. (*Oxycoccus palustris* Pers.) and *Vaccinium microcarpum* (Turcz. ex Rupr.) Schmalh. (*Oxycoccus microcarpus* Turcz. ex Rupr.). *J. Ecol.* **1997**, *85*, 381–396. [CrossRef]

9. Vander Kloet, S.P. *The Genus Vaccinium in North America*; Agriculture Canada: Ottawa, ON, Canada, 1988.
10. Bruederle, L.P.; Hugan, M.S.; Dignan, J.M.; Vorsa, N. Genetic Variation in Natural Populations of the Large Cranberry, *Vaccinium macrocarpon* Ait. (Ericaceae). *Bull. Torrey Bot. Club* **1996**, *123*, 41–47. [[CrossRef](#)]
11. Smith, T.W.; Walinga, C.; Wang, S.; Kron, P.; Suda, J.; Zalapa, J. Evaluating the relationship between diploid and tetraploid *Vaccinium oxycoccos* (Ericaceae) in eastern Canada. *Botany* **2015**, *93*, 623–636. [[CrossRef](#)]
12. Ballington, J.R. Collection, utilization, and preservation of genetic resources in *Vaccinium*. *HortScience* **2001**, *36*, 213–220. [[CrossRef](#)]
13. Song, G.-Q.; Hancock, J.F. *Vaccinium*. In *Wild Crop Relatives: Genomic and Breeding Resources: Temperate Fruits*; Kole, C., Ed.; Springer: Berlin/Heidelberg, Germany, 2011; pp. 197–221. ISBN 9783642160578.
14. Eaton, G.W.; Mahrt, B.J. Cold hardiness testing of cranberry flower buds. *Can. J. Plant Sci.* **1977**, *57*, 461–465. [[CrossRef](#)]
15. Ehlenfeldt, M.K.; Rowland, L.J.; Ogden, E.L.; Vinyard, B.T. Floral Bud Cold Hardiness of *Vaccinium ashei*, *V. constablaei*, and Hybrid Derivatives and the Potential for Producing Northern-adapted Rabbiteye Cultivars. *HortScience* **2007**, *42*, 1131–1134. [[CrossRef](#)]
16. Asada, T. Distribution of two taxa in *Vaccinium oxycoccus* sensu lato (Ericaceae) along micro-scale environmental gradients in Bekanbeushi Peatland, northern Japan. *Acta Phytotaxon. Geobot.* **2001**, *51*, 169–176.
17. Suda, J.; Lysák, M.A. A taxonomic study of the *Vaccinium* sect. *Oxycoccus* (Hill) WDJ Kock (Ericaceae) in the Czech Republic and adjacent territories. *Folia Geobot.* **2001**, *36*, 303–320. [[CrossRef](#)]
18. Camp, W.H. A Preliminary Consideration of the Biosystematy of *Oxycoccus*. *Bull. Torrey Bot. Club* **1944**, *71*, 426–437. [[CrossRef](#)]
19. Mahy, G.; Bruederle, L.P.; Connors, B.; Van Hofwegen, M.; Vorsa, N. Allozyme evidence for genetic autopolyploidy and high genetic diversity in tetraploid cranberry, *Vaccinium oxycoccos* (Ericaceae). *Am. J. Bot.* **2000**, *87*, 1882–1889. [[CrossRef](#)] [[PubMed](#)]
20. Soltis, D.E.; Soltis, P.S.; Rieseberg, L.H. Molecular Data and the Dynamic Nature of Polyploidy. *CRC Crit. Rev. Plant Sci.* **1993**, *12*, 243–273. [[CrossRef](#)]
21. Georgi, L.; Johnson-Cicalese, J.; Honig, J.; Das, S.P.; Rajah, V.D.; Bhattacharya, D.; Bassil, N.; Rowland, L.J.; Polashock, J.; Vorsa, N. The first genetic map of the American cranberry: Exploration of synteny conservation and quantitative trait loci. *Theor. Appl. Genet.* **2013**, *126*, 673–692. [[CrossRef](#)] [[PubMed](#)]
22. Covarrubias-Pazarán, G.; Diaz-García, L.; Schlautman, B.; Deutsch, J.; Salazar, W.; Hernandez-Ochoa, M.; Grygleski, E.; Steffan, S.; Iorizzo, M.; Polashock, J.; et al. Exploiting genotyping by sequencing to characterize the genomic structure of the American cranberry through high-density linkage mapping. *BMC Genom.* **2016**, *17*, 451. [[CrossRef](#)] [[PubMed](#)]
23. Daverdin, G.; Johnson-Cicalese, J.; Zalapa, J.; Vorsa, N.; Polashock, J. Identification and mapping of fruit rot resistance QTL in American cranberry using GBS. *Mol. Breed.* **2017**, *37*, 38. [[CrossRef](#)]
24. Schlautman, B.; Covarrubias-Pazarán, G. Development of a high-density cranberry SSR linkage map for comparative genetic analysis and trait detection. *Mol. Breed.* **2015**, *35*, 177. [[CrossRef](#)]
25. Schlautman, B.; Covarrubias-Pazarán, G.; Diaz-García, L.; Iorizzo, M.; Polashock, J.; Grygleski, E.; Vorsa, N.; Zalapa, J. Construction of a High-Density American Cranberry (*Vaccinium macrocarpon* Ait.) Composite Map Using Genotyping-by-Sequencing for Multi-pedigree Linkage Mapping. *G3* **2017**, *7*, 1177–1189. [[CrossRef](#)] [[PubMed](#)]
26. Diaz-García, L.; Covarrubias-Pazarán, G.; Schlautman, B.; Grygleski, E.; Zalapa, J. Image-based phenotyping for identification of QTL determining fruit shape and size in American cranberry (*Vaccinium macrocarpon* L.). *PeerJ* **2018**, *6*, e5461. [[CrossRef](#)] [[PubMed](#)]
27. Diaz-García, L.; Schlautman, B.; Covarrubias-Pazarán, G.; Maule, A.; Johnson-Cicalese, J.; Grygleski, E.; Vorsa, N.; Zalapa, J. Massive phenotyping of multiple cranberry populations reveals novel QTLs for fruit anthocyanin content and other important chemical traits. *Mol. Genet. Genom.* **2018**, *293*, 1379–1392. [[CrossRef](#)] [[PubMed](#)]
28. Polashock, J.; Zelzion, E.; Fajardo, D.; Zalapa, J.; Georgi, L.; Bhattacharya, D.; Vorsa, N. The American cranberry: First insights into the whole genome of a species adapted to bog habitat. *BMC Plant Biol.* **2014**, *14*, 165. [[CrossRef](#)] [[PubMed](#)]
29. Fajardo, D.; Senalik, D.; Ames, M.; Zhu, H.; Steffan, S.A.; Harbut, R.; Polashock, J.; Vorsa, N.; Gillespie, E.; Kron, K.; et al. Complete plastid genome sequence of *Vaccinium macrocarpon*: Structure, gene content, and rearrangements revealed by next generation sequencing. *Tree Genet. Genomes* **2013**, *9*, 489–498. [[CrossRef](#)]

30. Fajardo, D.; Schlautman, B.; Steffan, S.; Polashock, J.; Vorsa, N.; Zalapa, J. The American cranberry mitochondrial genome reveals the presence of selenocysteine (tRNA-Sec and SECIS) insertion machinery in land plants. *Gene* **2014**, *536*, 336–343. [[CrossRef](#)] [[PubMed](#)]
31. Zhu, H.; Senalik, D.; McCown, B.H.; Zeldin, E.L.; Speers, J.; Hyman, J.; Bassil, N.; Hummer, K.; Simon, P.W.; Zalapa, J.E. Mining and validation of pyrosequenced simple sequence repeats (SSRs) from American cranberry (*Vaccinium macrocarpon* Ait.). *Theor. Appl. Genet.* **2012**, *124*, 87–96. [[CrossRef](#)] [[PubMed](#)]
32. Zalapa, J.E.; Bougie, T.C.; Bougie, T.A.; Schlautman, B.J.; Wiesman, E.; Guzman, A.; Fajardo, D.A.; Steffan, S.; Smith, T. Clonal diversity and genetic differentiation revealed by SSR markers in wild *Vaccinium macrocarpon* and *Vaccinium oxycoccos*. *Ann. Appl. Biol.* **2015**, *166*, 196–207. [[CrossRef](#)]
33. Schlautman, B.; Bolivar-Medina, J.; Hodapp, S.; Zalapa, J. Cranberry SSR multiplexing panels for DNA horticultural fingerprinting and genetic studies. *Sci. Hortic.* **2017**, *219*, 280–286. [[CrossRef](#)]
34. Schlautman, B.; Fajardo, D.; Bougie, T.; Wiesman, E.; Polashock, J.; Vorsa, N.; Steffan, S.; Zalapa, J. Development and validation of 697 novel polymorphic genomic and EST-SSR markers in the American cranberry (*Vaccinium macrocarpon* Ait.). *Molecules* **2015**, *20*, 2001–2013. [[CrossRef](#)] [[PubMed](#)]
35. Schlautman, B.; Covarrubias-Pazarán, G.; Fajardo, D.; Steffan, S.; Zalapa, J. Discriminating power of microsatellites in cranberry organelles for taxonomic studies in *Vaccinium* and *Ericaceae*. *Genet. Resour. Crop Evol.* **2017**, *64*, 451–466. [[CrossRef](#)]
36. Koren, S.; Walenz, B.P.; Berlin, K.; Miller, J.R.; Bergman, N.H.; Phillippy, A.M. Canu: Scalable and accurate long-read assembly via adaptive k-mer weighting and repeat separation. *Genome Res.* **2017**, *27*, 722–736. [[CrossRef](#)] [[PubMed](#)]
37. Hunt, M.; Silva, N.D.; Otto, T.D.; Parkhill, J.; Keane, J.A.; Harris, S.R. Circlator: Automated circularization of genome assemblies using long sequencing reads. *Genome Biol.* **2015**, *16*, 294. [[CrossRef](#)] [[PubMed](#)]
38. Tillich, M.; Lehwark, P.; Pellizzer, T.; Ulbricht-Jones, E.S.; Fischer, A.; Bock, R.; Greiner, S. GeSeq—Versatile and accurate annotation of organelle genomes. *Nucleic Acids Res.* **2017**, *45*, W6–W11. [[CrossRef](#)] [[PubMed](#)]
39. Kearse, M.; Moir, R.; Wilson, A.; Stones-Havas, S.; Cheung, M.; Sturrock, S.; Buxton, S.; Cooper, A.; Markowitz, S.; Duran, C.; et al. Geneious Basic: An integrated and extendable desktop software platform for the organization and analysis of sequence data. *Bioinformatics* **2012**, *28*, 1647–1649. [[CrossRef](#)] [[PubMed](#)]
40. R Core Team. *R: A Language and Environment for Statistical Computing*; R Foundation for Statistical Computing: Vienna, Austria, 2013.
41. Mayer, C. Phobos, a tandem repeat search tool for complete genomes. *Version* **2008**, *3*, 12.
42. Bolger, A.M.; Lohse, M.; Usadel, B. Trimmomatic: A flexible trimmer for Illumina sequence data. *Bioinformatics* **2014**, *30*, 2114–2120. [[CrossRef](#)]
43. Darling, A.C.E.; Mau, B.; Blattner, F.R.; Perna, N.T. Mauve: Multiple alignment of conserved genomic sequence with rearrangements. *Genome Res.* **2004**, *14*, 1394–1403. [[CrossRef](#)] [[PubMed](#)]
44. Katoh, K.; Standley, D.M. MAFFT multiple sequence alignment software version 7: Improvements in performance and usability. *Mol. Biol. Evol.* **2013**, *30*, 772–780. [[CrossRef](#)]
45. Price, M.N.; Dehal, P.S.; Arkin, A.P. FastTree 2—Approximately maximum-likelihood trees for large alignments. *PLoS ONE* **2010**, *5*, e9490. [[CrossRef](#)] [[PubMed](#)]
46. Delcher, A.L.; Salzberg, S.L.; Phillippy, A.M. Using MUMmer to identify similar regions in large sequence sets. *Curr. Protoc. Bioinform.* **2003**, *10*. [[CrossRef](#)] [[PubMed](#)]
47. Hisano, H.; Tsujimura, M.; Yoshida, H.; Terachi, T.; Sato, K. Mitochondrial genome sequences from wild and cultivated barley (*Hordeum vulgare*). *BMC Genom.* **2016**, *17*, 824. [[CrossRef](#)] [[PubMed](#)]
48. Yukawa, M.; Tsudzuki, T.; Sugiura, M. The chloroplast genome of *Nicotiana sylvestris* and *Nicotiana tomentosiformis*: Complete sequencing confirms that the *Nicotiana sylvestris* progenitor is the maternal genome donor of *Nicotiana tabacum*. *Mol. Genet. Genom.* **2006**, *275*, 367–373. [[CrossRef](#)] [[PubMed](#)]
49. Bi, C.; Paterson, A.H.; Wang, X.; Xu, Y.; Wu, D.; Qu, Y.; Jiang, A.; Ye, Q.; Ye, N. Analysis of the Complete Mitochondrial Genome Sequence of the Diploid Cotton *Gossypium raimondii* by Comparative Genomics Approaches. *Biomed Res. Int.* **2016**, *2016*, 5040598. [[CrossRef](#)] [[PubMed](#)]
50. Handa, H. The complete nucleotide sequence and RNA editing content of the mitochondrial genome of rapeseed (*Brassica napus* L.): Comparative analysis of the mitochondrial genomes of rapeseed and *Arabidopsis thaliana*. *Nucleic Acids Res.* **2003**, *31*, 5907–5916. [[CrossRef](#)]

51. Oda, K.; Yamato, K.; Ohta, E.; Nakamura, Y.; Takemura, M.; Nozato, N.; Akashi, K.; Ohyama, K. Transfer RNA genes in the mitochondrial genome from a liverwort, *Marchantia polymorpha*: The absence of chloroplast-like tRNAs. *Nucleic Acids Res.* **1992**, *20*, 3773–3777. [[CrossRef](#)] [[PubMed](#)]
52. Ye, N.; Wang, X.; Li, J.; Bi, C.; Xu, Y.; Wu, D.; Ye, Q. Assembly and comparative analysis of complete mitochondrial genome sequence of an economic plant *Salix suchowensis*. *PeerJ* **2017**, *5*, e3148. [[CrossRef](#)]
53. Rose, J.P.; Kleist, T.J.; Löfstrand, S.D.; Drew, B.T.; Schönenberger, J.; Sytsma, K.J. Phylogeny, historical biogeography, and diversification of angiosperm order Ericales suggest ancient Neotropical and East Asian connections. *Mol. Phylogenet. Evol.* **2018**, *122*, 59–79. [[CrossRef](#)] [[PubMed](#)]
54. Szczecinska, M.; Gomolinska, A.; Szkudlarz, P.; Sawicki, J. Plastid and nuclear genomic resources of a relict and endangered plant species: *Chamaedaphne calyculata* (L.) Moench (Ericaceae). *Turk. J. Bot.* **2014**, *38*, 1229–1238. [[CrossRef](#)]
55. Bartsch, I. Effects of fertilization on growth and nutrient use by *Chamaedaphne calyculata* in a raised bog. *Can. J. Bot.* **1994**, *72*, 323–329. [[CrossRef](#)]
56. Guisinger, M.M.; Kuehl, J.V.; Boore, J.L.; Jansen, R.K. Extreme reconfiguration of plastid genomes in the angiosperm family Geraniaceae: Rearrangements, repeats, and codon usage. *Mol. Biol. Evol.* **2011**, *28*, 583–600. [[CrossRef](#)] [[PubMed](#)]
57. Heintzman, P.D.; Froese, D.; Ives, J.W.; Soares, A.E.R.; Zazula, G.D.; Letts, B.; Andrews, T.D.; Driver, J.C.; Hall, E.; Hare, P.G.; et al. Bison phylogeography constrains dispersal and viability of the Ice Free Corridor in western Canada. *Proc. Natl. Acad. Sci. USA* **2016**, *113*, 8057–8063. [[CrossRef](#)] [[PubMed](#)]
58. Porsild, A.E. Earth Mounds in Unglaciaded Arctic Northwestern America. *Geogr. Rev.* **1938**, *28*, 46–58. [[CrossRef](#)]



© 2019 by the authors. Licensee MDPI, Basel, Switzerland. This article is an open access article distributed under the terms and conditions of the Creative Commons Attribution (CC BY) license (<http://creativecommons.org/licenses/by/4.0/>).